On the intrinsic shape of gamma-ray spectrum for Fermi blazars *

Shi-Ju Kang^{1,2,*}, Qingwen Wu³, Yong-Gang Zheng⁴, Yue Yin¹, Jia-Li Song¹, Hang Zou¹, Jian-Chao Feng^{5,2}, Ai-Jun Dong^{5,2}, Zhong-Zu Wu⁶, Zhi-Bin Zhang⁶, Lin-Hui Wu³

- ¹ School of Electrical Engineering, Liupanshui Normal University, Liupanshui, Guizhou, 553004, China; *kangshiju@hust.edu.cn*
- ² Guizhou Provincial Key Laboratory of Radio Astronomy and Data Processing;
- ³ School of Physics, Huazhong University of Science and Technology, Wuhan, Hubei, 430074, China; *qwwu@hust.edu.cn*
- ⁴ Department of Physics, Yunnan Normal University, Kunming, Yunnan, 650092, China; ynzgy@ynu.edu.cn
- ⁵ School of Physics and Electronic Science, Guizhou Normal University, Guiyang, 550001, China; fengjc@gznu.edu.cn
- ⁶ Department of Physics, College of Science, Guizhou University, Guiyang 550025, China.

Received October 10, 2017; accepted February 10, 2018

Abstract The curvature of the γ -ray spectrum in blazars may reflect the intrinsic distribution of the emitting electron distribution, which will further give some information on the possible acceleration and cooling processes in the emitting region. The γ -ray spectra of Fermi blazars are normally fitted either by a single power-law (PL) or a log-normal (call Logarithmic Parabola, LP) form. The possible reason for this difference is not unclear. We statistically explore this issue based on the different observational properties of 1419 Fermi blazars in the 3LAC Clean sample. We find that the γ -ray flux (100 MeV-100 GeV) and variability index follow bimodal distributions for PL and LP blazars, where γ -ray flux and variability index show a positive correlation. However, the distributions of the γ -ray luminosity and redshift follow a unimodal distribution. Our results suggest that the bimodal distribution of γ -ray flux for LP and PL blazars may be not intrinsic and all blazars may have an intrinsic curved γ -ray spectrum and the PL spectrum is just caused by the fitting effect due to the less photons.

Key words: galaxies: active - galaxies: jets - gamma rays: galaxies - galaxies: statistics

1 INTRODUCTION

Blazars, including flat-spectrum radio quasars (FSRQs) and BL Lacertae objects (BL Lacs), are most powerful active galactic nucleis (AGNs) with a relativistic jet orientated at a small viewing angle to the line of sight (Urry & Padovani 1995), which show rapid variability and high luminosity, high and variable polarization, superluminal motions, core-dominated non-thermal continuum and strong γ -ray emissions, etc (Zhang et al. 2002; Abdo et al. 2010b; Gu & Li 2013; Fan et al. 2016a; Wagner & Witzel 1995; Andruchow et al. 2005; Jorstad et al. 2005). The multi-wavelength spectral energy distribution (SED) from the radio to the γ -ray bands of blazars dominantly come from the non-thermal emission, where the SED normally exhibits a two-hump structure in the $log\nu - log\nu F_{\nu}$ space. Location of the peak for the lower energy bump in the SED, ν_p^S , blazars are used to classify the sources as low (LSP, e.g., $\nu_p^S < 10^{14}$ Hz), intermediate (ISP, e.g., 10^{14} Hz $< \nu_p^S < 10^{15}$ Hz) and high-synchrotron-peaked (HSP, e.g., $\nu_p^S > 10^{15}$ Hz) blazars (e.g., Abdo et al. 2010b). BL Lacs show a wide distribution (LSP, ISP and HSP), however, almost all FSRQs are LSP blazars.

It is generally acknowledged that the lower-energy hump is normally attributed to the synchrotron emission produced by the non-thermal relativistic electrons in the jet (Urry 1998), while the origin of the second hump is still an open issue. In the leptonic model scenarios, the high-energy γ -rays mainly come from inverse Compton (IC) scattering of the relativistic electrons either on the synchrotron photons inside the jet (synchrotron self-Compton, SSC, process; e.g., Maraschi et al. 1992; Bloom & Marscher 1996; Mastichiadis & Kirk 1997; Konopelko et al. 2003) and/or on some other photon populations from outside the jet (external-Compton, EC, process, e.g., Dermer et al. 1992; Dermer & Schlickeiser 1993; Sikora et al. 1994; Ghisellini & Madau 1996; Böttcher & Dermer 1998). And the hadron model considers that the highenergy γ -ray emission originates from the synchrotron radiation process of extremely relativistic protons (Aharonian 2000; Mücke & Protheroe 2001; Mücke et al. 2003; Petropoulou 2014), or the cascade process of the proton-proton or proton-photon interactions (e.g., Mannheim & Biermann 1992; Mannheim 1993; Pohl & Schlickeiser 2000; Atoyan & Dermer 2001; Zheng & Kang 2013; Cao & Wang 2014; Yan & Zhang 2015; Zheng et al. 2016).

The third Fermi Large Area Telescope (LAT) source catalog (3FGL) is now available (Acero et al. 2015). The 3FGL catalog includes 3033 γ -ray sources: 2192 high-latitude and 841 low-latitude γ -ray sources, where most sources (1717) belong to blazars (Ackermann et al. 2015). Based on the 3FGL (Acero et al. 2015), the third catalog of AGNs detected by the Fermi-LAT (3LAC) is presented (Ackermann et al. 2015). The high-confidence clean sample of the 3LAC (3LAC Clean Sample), using the first four years of the Fermi-LAT data, lists 1444 γ -ray AGNs (Ackermann et al. 2015), which includes 414 FSRQs (\sim 30%), 604 BL Lac objects (\sim 40%), 402 blazars candidates of uncertain type (BCUs, \sim 30%) and 24 non-blazar AGNs (< 2%). It is a good chance to study the nature for γ -ray emissions of blazars using the such a large sample of Fermi-LAT blazars. The physical properties of blazars have been extensive sample researched based on the Fermi source catalogs (e.g., Fan et al. 2016; King 4 catalog; King 2016; King & Zhang 2014; Lin et al. 2017; Chen et al. 2016; Singal et al. 2012; Singal 2015). The γ -ray spectrum of the Fermi-LAT blazars in 3FGL catalog mainly exhibits two different spectral shapes: Logarithmic Parabola (LP) and Power Law (PL) shapes γ -

hints on the formation mechanisms of the high-energy electron spectrum in the jet (e.g., Landau et al. 1986; Tramacere et al. 2007, 2009; Massaro et al. 2004a; Yan et al. 2013; Chen 2014; Massaro et al. 2006; Paggi et al. 2009; Massaro et al. 2016; Fan et al. 2016a). In this work, we aim to find (only focus on) the observational differences for the blazars with LP and PL γ -ray spectrum through the statistical analyses on the 3LAC Clean Sample. We give some description on the sample selection in Section 2, and the results are shown in Section 3. The discussion and conclusion are presented in Section 4.

2 SAMPLE

The 3LAC Clean Sample lists 1444 γ -ray AGNs (Ackermann et al. 2015) with 414 FSRQs, 604 BL Lac objects, 402 BCU blazars and 24 non-blazar AGNs. We select 1419 Fermi blazars from 3LAC Clean Sample (3C 454.3 fitted with an exponentially cutoff power law is neglected). In this sample, the spectra of 130 sources are fitted with LP and that of 1289 sources are fitted with PL. In table 1, we present the 3FGL Fermi names, redshift, optical classifications (BL Lac and FSRQ, or BCUs), γ -ray spectral shape (LP and PL) for selected blazars from the 3LAC Website version¹. In addition, we also collect their variability index², γ -ray energy flux (S_{γ}, from 100 MeV to 100 GeV obtained by spectrum fitting) from the 3FGL. The γ -ray luminosity (L $_{\gamma}$) is calculated with $\nu L_{\gamma} = 4\pi D_L^2 \nu S_{\gamma,corr}$, where D_L is the luminosity distance³. The γ -ray energy fluxes, S_{γ} , of PL γ -ray spectrum in the source rest frame are K-corrected with the formula $S_{\gamma,corr} = S_{\gamma,obs}(1+z)^{\alpha-1}$ (e.g., Lin & Fan 2016; Mao et al. 2016), where z is the redshift, α is the spectral index ($\alpha = \Gamma_{\rm ph} - 1$, α comes from the $\Gamma_{\rm ph}$ values, $\Gamma_{\rm ph}$ is power-law photon index, where $dN/dE = K(E/E_0)^{-\Gamma}$ (Acero et al. 2015). For LP type of γ -ray spectrum blazars, the γ -ray flux are calculated using a modified K-correction according to its spectral shape $S_{\gamma,corr} = S_{\gamma,obs}(1+z)^{1-\alpha'-\beta\log(1+z)}$ (see Mao et al. 2016 for the details and references therein), β is curvature parameter, α' is obtained from fitting the γ -ray spectrum using a log parabola instead of the usual power law, where $dN/dE = K(E/E_0)^{-\alpha'-\beta \log E/E_0}$ (Acero et al. 2015). In this sample, there are 759 sources with the measured redshift (109 LP sources and 650 PL sources). The γ -ray luminosity are also listed in Table 1.

3 RESULTS

We present the statistical results in Figures 1 and 2 , where the correlations and histograms are shown for both PL and LP blazars. From the correlations of variability index-S_{γ} and variability index-L_{γ}, we find that the LP sources normally have higher γ -ray flux and variability index compared the PL sources (top left panel of Figure 1), where the variability index and S_{γ} show a positive correlation with a Pearson correlation coefficients of 0.81. The histograms of both variability index and γ -ray flux are shown evident bimodal distributions for LP and PL sources (top panels in Figure 2), where the KMM-test (see Ashman et al. 1994 for the details and references therein) strongly reject that LP and PL sources follow a unimodal distribution (probabilities are $1.0 \times 10^{-\infty}$ and 1.25×10^{-33} for variability index and S_{γ} respectively). The bimodal

¹ http://www.asdc.asi.it/fermi3lac/

² Sum of $2 \times \log(\text{Likelihood})$ difference between the flux fitted in each time interval and the average flux over the full catalog interval, see Table 16 in Acero et al. (2015).

S.-J. Kang et al.

3FGL name	Optical class	Spectral type	Z	S_{γ}	VI	$\log L_{\gamma}$
3FGL J0001.2-0748	BL Lac	PL		7.82E-12	49.74	
3FGL J0001.4+2120	FSRQ	LP	1.106	8.07E-12	130.34	46.27
3FGL J0002.2-4152	BCU	PL		3.02E-12	56.35	
3FGL J0003.2-5246	BCU	PL		3.01E-12	45.28	
3FGL J0004.7-4740	FSRQ	PL	0.880	9.19E-12	112.93	46.67
3FGL J0006.4+3825	FSRQ	PL	0.229	1.04E-11	80.46	45.27
3FGL J0008.0+4713	BL Lac	PL	2.100	2.19E-11	36.71	47.89
3FGL J0008.6-2340	BL Lac	PL	0.147	3.47E-12	47.35	44.28
:	:	:	:	:	:	:
•	•	•	•	•	•	•

Table 1: Data of sample

Note—Columns 1 is the 3FGL names; Columns 2 lists the optical class; Columns 3 gives the gamma-ray spectral type; Column 4 is redshift; Column 5 gives the energy flux ($S_{\gamma} \text{ erg cm}^{-2} \text{ s}^{-1}$); The variability index (VI) is listed in column 6; Columns 7 reports the gamma-ray luminosity ($L_{\gamma} \text{ erg s}^{-1}$) with a measured redshift.

(This table is available in its entirety in xls format.)

Table 2: Probabilities of KMM-test

probabilities	S_γ	VI	Z	L_{γ}
р	$1.0\times 10^{-\infty}$	1.25×10^{-33}	0.995	0.999

distributions remain unchanged, even only consider the sources with known redshift (the blue lines and dash lines in top panels in Figure 2).

From the correlations of Variability index-redshift and S_{γ} -redshift, we find that both LP and PL sources do not well correlated with the redshift. The KMM-test also show that there is roughly no difference for LP and PL sources in the histogram of redshift, where the probability is p = 0.995 and reject the bimodal distribution of redshift for these two populations. In the correlations of γ -ray flux-redshift and γ -ray luminosity-redshift, we can find that there are no differences in the distributions of redshift and γ -ray luminosity for LP and PL sources even though LP sources normally have the higher fluxes compared the PL sources. We also show the histogram of γ -ray luminosity for both LP and PL sources in bottom-right panel of Figure 2, where these two populations should follow a unimodal distribution with a KMM-test probability of p = 0.999. In the correlation of γ -ray flux- γ -ray luminosity, we find that the bright sources with higher γ -ray flux show LP shape γ -ray spectrum (e.g. Nolan et al. 2012).

4 DISCUSSIONS ANG CONCLUSIONS

Based on the 3LAC Clean Sample, we compile to 1419 Fermi blazars with 4 different parameters: variability index, γ -ray energy flux, γ -ray luminosity and redshift. We explore the possible differences between LP and PL blazars based on the simple statistical analyses on these parameters. We find that the distributions of variability index and γ -ray flux are evidently different for the subsamples of LP and PL blazars (Figures 1 and 2). However, we don't find evident differences in the distributions of γ -ray luminosity and redshift for LP and PL blazars. Our above conclusions remain unchanged for different optical classes (e.g., for the

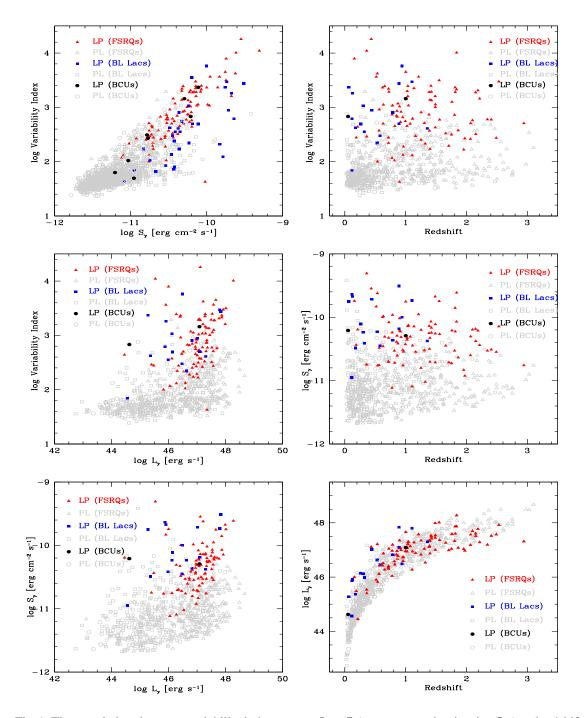


Fig. 1: The correlations between variability index, energy flux (S_{γ}) , gamma-ray luminosity (L_{γ}) and redshift for blazars. The red solid triangles, blue squares and black points indicate the observational data for FSRQs, BL Lacs and BCU blazars with the LP shape γ -ray spectrum; The grey empty triangles, squares and points represent the observational data for FSRQs, BL Lacs and BCU blazars with the PL shape γ -ray spectrum.

The unimodal distribution of γ -ray luminosity and bimodal distributions of variability index and γ ray flux for LP and PL blazars may suggest that these two type of difference may be are observational effect and the γ -ray spectrum of all sources may be curved if we can detect more γ -ray photons. The γ -ray spectral shape of Fermi blazars can shed light on the possible intrinsic physics on the jet physics. For example, the emitting electron energy distribution (EED) can be determined by the modeling the

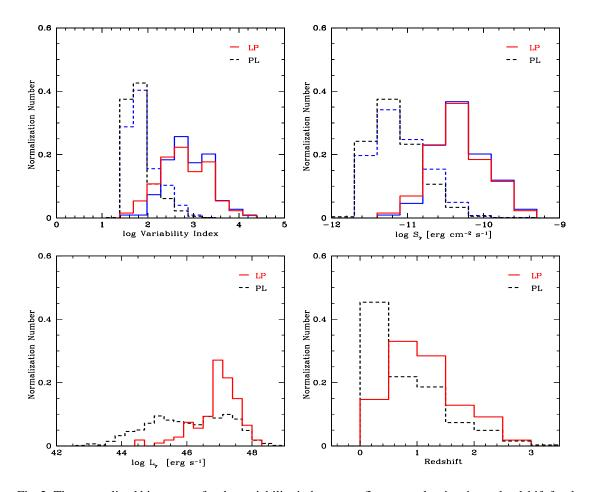


Fig. 2: The normalized histograms for the variability index, γ -ray flux, γ -ray luminosity and redshift for the selected sources, where solid and dashed lines represent of LP and PL shape of γ -ray spectrum respectively. In the up panels, the blue lines and dash lines indicate the results for the sources with known redshift.

Kang et al. 2011, 2012; Abdo et al. 2010a; Paggi et al. 2009; Massaro et al. 2004a,b, 2006; Chen 2014). The form of the EED can give further information on the acceleration and cooling processes. First-order Fermi acceleration (shock acceleration) can naturally reproduce the PL EED (e.g., Drury 1983; Drury & Falle 1986; Axford et al. 1977; Drury et al. 1999; Krymskii 1977; Bell 1978a,b; Blandford & Ostriker 1978; Kirk et al. 1998). Second-order Fermi particle acceleration (stochastic acceleration) can form LP EED in the case of the acceleration process dominating over the radiative cooling (e.g., Massaro et al. 2004a,b, 2006; Becker et al. 2006; Tramacere et al. 2011). If there is no acceleration process in the emitting region, the cooled EED is the broken PL shape (e.g., Chiaberge & Ghisellini 1999). Furthermore, it is found that the curvature of the spectrum may related to the peak frequency of the first hump in the SED of blazars, which seem to support the stochastic particle accelerations (e.g., Chen 2014). The intrinsic curved γ -ray spectrum may be induced by the curved EED coming from the stochastic acceleration process, or stochastic dominating acceleration process (e.g., Lewis et al. 2018). It should be noted that the extragalactic background light (EBL) might play a role in the curvature of the gamma-ray spectra altering the intrinsic blazars spectral shape. This will impact the conclusions on the intrinsic particle distribution in blazar jets (e.g., It is also important to note that the BCU blazars and/or without distance information might be biased towards BL Lac objects as the absence of spectral line features is a major hurdle in their identification and distance measurements. This is mandatory to exclude selection effects that can enter the statistical analyses of the parameter spaces thereby affecting conclusions on the jet physics of the Fermi-LAT blazars. The fainter and brighter sets of sources follow broader and more overlapping ranges in luminosity and redshift than they do in their flux. Such analysis would require issues of redshift completeness to be addressed , and the application of sophisticated statistical tools.

In this work, in addition, we merely takes a published Fermi catalogue and makes various X-Y and histogram plots, adding no external data, and have not done any of the fittings ourselves; only based on these data obtained from Fermi catalogue, for the limited parameters, via a simple statistical Analysis (e.g.,bimodality test), to explore the intrinsic gamma-ray spectrum of Fermi blazar by compared the LP and PL blazars, which suggest a obvious inference that the fainter sources could be more complex in their properties — more complex analysis is inhibited by the fact they are fainter sources. This result could be some bias, due to the simple statistical approach, the limited sample and the source of the sample data (obtained from the Fermi catalogue fitted by the Fermi team). The more preferable statistical approach, the big and completeness sample data, the more parameters (e.g., the mass of central black hole, and/or the polarization information of the jet radiation, etc.), and the sophisticated fitting analysis are needed to further address the intrinsic jet physics of Fermi-LAT blazars.

Acknowledgements We thank the anonymous referee for very constructive and helpful comments and suggestions, which greatly helped us to improve our paper. This work is supported by the National Natural Science Foundation of China (NSFC: 11763005, 11622324, 11573009, 11763002, U1431111, and U1431126). This work is aslo supported by the Research Foundation for Advanced Talents of Liupanshui Normal University (LPSSYKYJJ201506), the Open Fund of Guizhou Provincial Key Laboratory of Radio Astronomy and Data Processing, the Physical Electronic Key Discipline of Guizhou Province (ZDXK201535), the Natural Science Foundation of the Department of Education of Guizhou Province (QJHKYZ[2015]455) and the Research Foundation of Liupanshui Normal University (LPSSYDXS1514, LPSSY201401).

References

Abdo, A. A., Ackermann, M., Agudo, I., et al. 2010a, ApJ, 721, 1425 6
Abdo, A. A., Ackermann, M., Agudo, I., et al. 2010b, ApJ, 716, 30 2
Acero, F., Ackermann, M., Ajello, M., et al. 2015, ApJS, 218, 23 2, 3
Ackermann, M., Ajello, M., Atwood, W. B., et al. 2015, ApJ, 810, 14 2, 3
Aharonian, F. A. 2000, New Astron., 5, 377 2
Aleksić, J., Ansoldi, S., Antonelli, L. A., et al. 2015, MNRAS, 450, 4399 6
Andruchow, I., Romero, G. E., & Cellone, S. A. 2005, A&A, 442, 97 2
Ashman, K. M., Bird, C. M., & Zepf, S. E. 1994, AJ, 108, 2348 3
Atoyan, A., & Dermer, C. D. 2001, Physical Review Letters, 87, 221102 2

- Becker, P. A., Le, T., & Dermer, C. D. 2006, ApJ, 647, 539 6
- Bell, A. R. 1978a, MNRAS, 182, 147 6
- Bell, A. R. 1978b, MNRAS, 182, 443 6
- Blandford, R. D., & Ostriker, J. P. 1978, ApJ, 221, L29 6
- Bloom, S. D., & Marscher, A. P. 1996, ApJ, 461, 657 2
- Böttcher, M., & Dermer, C. D. 1998, ApJ, 501, L51 2
- Cao, G., & Wang, J. 2014, ApJ, 783, 108 2
- Cerruti, M., Dermer, C. D., Lott, B., Boisson, C., & Zech, A. 2013, ApJ, 771, L4 5
- Chen, L. 2014, ApJ, 788, 179 3, 6
- Chen, Y.-Y., Zhang, X., Xiong, D.-R., Wang, S.-J., & Yu, X.-L. 2016, RAA (Research in Astronomy and Astrophysics), 16, 13 2
- Chiaberge, M., & Ghisellini, G. 1999, MNRAS, 306, 551 6
- Dermer, C. D., & Schlickeiser, R. 1993, ApJ, 416, 458 2
- Dermer, C. D., Schlickeiser, R., & Mastichiadis, A. 1992, A&A, 256, L27 2
- Drury, L. O. 1983, Reports on Progress in Physics, 46, 973 6
- Drury, L. O., Duffy, P., Eichler, D., & Mastichiadis, A. 1999, A&A, 347, 370 6
- Drury, L. O., & Falle, S. A. E. G. 1986, MNRAS, 223, 353 6
- Fan, J. H., Yang, J. H., Liu, Y., et al. 2016a, ApJS, 226, 20 2, 3
- Fan, X.-L., Bai, J.-M., & Mao, J.-R. 2016b, RAA (Research in Astronomy and Astrophysics), 16, 173 2
- Ghisellini, G. 2016, Galaxies, 4, 36 2
- Ghisellini, G., & Madau, P. 1996, MNRAS, 280, 67 2
- Gu, M. F., & Li, S.-L. 2013, A&A, 554, A51 2
- Jorstad, S. G., Marscher, A. P., Lister, M. L., et al. 2005, AJ, 130, 1418 2
- Kang, S. J., Huang, B. R., Kang, T., Liang, J. H., & Zheng, Y. G. 2011, Acta Astronomica Sinica, 52, 357 6
- Kang, S.-j., Huang, B.-r., Kang, T., Liang, J.-h., & Zheng, Y.-g. 2012, Chinese Astronomy and Astrophysics, 36, 115 6
- Kirk, J. G., Rieger, F. M., & Mastichiadis, A. 1998, A&A, 333, 452 6
- Konopelko, A., Mastichiadis, A., Kirk, J., de Jager, O. C., & Stecker, F. W. 2003, ApJ, 597, 851 2
- Krymskii, G. F. 1977, Soviet Physics Doklady, 22, 327 6
- Landau, R., Golisch, B., Jones, T. J., et al. 1986, ApJ, 308, 78 3, 5
- Lewis, T. R., Finke, J. D., & Becker, P. A. 2018, ApJ, 853, 6 6
- Lin, C., & Fan, J.-H. 2016, RAA (Research in Astronomy and Astrophysics), 16, 103 2, 3
- Lin, C., Fan, J.-H., & Xiao, H.-B. 2017, RAA (Research in Astronomy and Astrophysics), 17, 066 2
- Mannheim, K. 1993, A&A, 269, 67 2
- Mannheim, K., & Biermann, P. L. 1992, A&A, 253, L21 2
- Mao, P., Urry, C. M., Massaro, F., et al. 2016, ApJS, 224, 26 2, 3
- Maraschi, L., Ghisellini, G., & Celotti, A. 1992, ApJ, 397, L5 2
- Massaro, E., Perri, M., Giommi, P., & Nesci, R. 2004a, A&A, 413, 489 3, 6
- Massaro, E., Perri, M., Giommi, P., Nesci, R., & Verrecchia, F. 2004b, A&A, 422, 103 6

- Massaro, E., Tramacere, A., Perri, M., Giommi, P., & Tosti, G. 2006, A&A, 448, 861 3, 6
- Massaro, F., Thompson, D. J., & Ferrara, E. C. 2016, A&A Rev., 24, 2 3
- Mastichiadis, A., & Kirk, J. G. 1997, A&A, 320, 19 2
- Mücke, A., & Protheroe, R. J. 2001, Astroparticle Physics, 15, 121 2
- Mücke, A., Protheroe, R. J., Engel, R., Rachen, J. P., & Stanev, T. 2003, Astroparticle Physics, 18, 593 2
- Nolan, P. L., Abdo, A. A., Ackermann, M., et al. 2012, ApJS, 199, 31 4
- Paggi, A., Massaro, F., Vittorini, V., et al. 2009, A&A, 504, 821 3, 6
- Petropoulou, M. 2014, MNRAS, 442, 3026 2
- Pohl, M., & Schlickeiser, R. 2000, A&A, 354, 395 2
- Sikora, M., Begelman, M. C., & Rees, M. J. 1994, ApJ, 421, 153 2
- Singal, J. 2015, MNRAS, 454, 115 2
- Singal, J., Petrosian, V., & Ajello, M. 2012, ApJ, 753, 45 2
- Tramacere, A., Giommi, P., Perri, M., Verrecchia, F., & Tosti, G. 2009, A&A, 501, 879 3, 5
- Tramacere, A., Massaro, E., & Taylor, A. M. 2011, ApJ, 739, 66 6
- Tramacere, A., Massaro, F., & Cavaliere, A. 2007, A&A, 466, 521 3, 5
- Urry, C. M. 1998, Advances in Space Research, 21, 89 2
- Urry, C. M., & Padovani, P. 1995, PASP, 107, 803 2
- Wagner, S. J., & Witzel, A. 1995, ARA&A, 33, 163 2
- Xiong, D. R., & Zhang, X. 2014, MNRAS, 441, 3375 2
- Yan, D., & Zhang, L. 2015, MNRAS, 447, 2810 2
- Yan, D., Zhang, L., Yuan, Q., Fan, Z., & Zeng, H. 2013, ApJ, 765, 122 3, 5
- Zhang, L. Z., Fan, J.-H., & Cheng, K.-S. 2002, PASJ, 54, 159 2
- Zheng, Y. G., & Kang, T. 2013, ApJ, 764, 113 2
- Zheng, Y. G., Yang, C. Y., & Kang, S. J. 2016, A&A, 585, A8 2